Chemical Engineering Science 156 (2016) 147–161

Contents lists available at ScienceDirect

Chemical Engineering Science

journal homepage: www.elsevier.com/locate/ces

Experimental study of the hydrodynamic behaviour of slug flow in a horizontal pipe

M. Abdulkadir [a,b,*], V. Hernandez-Perez [c,d], I.S. Lowndes [c], B.J. Azzopardi [c], E. Sam-Mbomah [b]

[a] Department of Chemical Engineering, Federal University of Technology, Minna, Niger State, Nigeria
[b] Petroleum Engineering Department, African University of Science and Technology (AUST), Abuja, Nigeria
[c] Process and Environmental Engineering Research Division, Faculty of Engineering, University of Nottingham, University Park, Nottingham NG7 2RD, United Kingdom
[d] Department of Mechanical Engineering, Faculty of Engineering, National University of Singapore, Singapore

HIGHLIGHTS

- Advanced instrumentation for slug flow measurement, namely ECT, under laboratory conditions, is used on a horizontal pipe
- In this study, oil with viscosity five times higher than water is used, as it is more relevant to industry
- Comparison with void fraction in the liquid slug and slug frequency data available in literature shows similar trends.
- Use of plots of average slug frequency against axial distance, probability density function (PDF) of void fraction and comparison of slug front and slug tail to establish flow development.

ARTICLE INFO

Article history:
Received 6 July 2016
Received in revised form
6 September 2016
Accepted 10 September 2016
Available online 20 September 2016

Keywords:
Air–silicone oil
ECT
Elongated bubble
Liquid slug
Frequency
Void fraction

ABSTRACT

This paper investigates the unsteady hydrodynamic behaviour of slug flow occurring within an air–silicone oil mixture, within a horizontal 67 mm internal diameter pipe. A series of slug flow regime experiments were performed for a range of injected air superficial velocities (0.29–1.4 m s−1) and for liquid flows with superficial velocities of between 0.05–0.47 m s−1. A pair of Electrical Capacitance Tomography (ECT) probes was used to determine: the slug translational velocities of the elongated bubbles and liquid slugs, the slug frequencies, the lengths of elongated bubbles and the liquid slugs, the void fractions within the elongated bubbles and liquid slugs. The pressure drop experienced along the pipe was measured using a differential pressure transducer cell (DP cell). A comparative analysis of the current experimental data and that previously published experimental confirms good agreement.

1. Introduction

Slug flows are the most prevalent and complex flow patterns experienced in multiphase transportation pipelines due to the long transport distances involved, and large pipeline diameters and uneven elevation profiles experienced in pipelines both onshore and offshore. As offshore production moves into deeper waters farther offshore, the cost of constructing and operating fixed platforms with separation facilities becomes increasingly challenging. An alternative solution is to utilize subsea production systems which entail minimum offshore processing. The presence of long, high density, fast moving liquid slugs within transport pipelines can cause significant variations in oil and gas flow rates entering downstream processing facilities, and result in mechanical damage to pipeline connections and supports (Bagci, 2003). Thus, an accurate prediction of the multiphase flow characteristics that may be experienced within these pipelines is therefore required to affect the safe and economic design and operation of these transportation systems. For this reason, it is of major interest within many industrial processes, including: upstream and downstream oil and gas processes, geothermal production of steam, chemical plants and refineries, and the handling and transport of cryogenic fluids (Bagci, 2003).

The literature is awash with large experimental data concerned with air–water flow in horizontal pipes and such data have been

* Corresponding author at: Department of Chemical Engineering, Federal University of Technology, Minna, Niger State, Nigeria.
E-mail address: mukhau@futminna.edu.ng (M. Abdulkadir).

http://dx.doi.org/10.1016/j.ces.2016.09.015
0009-2509/

used extensively in the development of many of the available models and correlations. Expectedly, engineers dealing with fluid typical of industrial applications complain that water has inappropriate values of physical properties, particularly a viscosity that is much smaller than many of the materials they deal with. The range of viscosity of oils in real systems is 2.63×10^{-3} to 1000×10^{-3} Pa s, respectively.

In addition, detailed descriptions of the flow phenomena for this flow regime are sparse. New developments in flow measurement and instrumentation are a way to move forward. For instance, Abdulkadir et al. (2014) carried out a detailed experimental investigation to study the hydrodynamics of slug flows in a 67 mm internal diameter vertical riser. They employed electrical capacitance tomography (ECT) transducer to determine: the translational velocities of the Taylor bubbles and liquid slugs, the slug frequencies, the lengths of the Taylor bubbles and the liquid slugs, the void fractions within the Taylor bubbles and liquid slugs and the liquid film thickness. Their study also used a differential pressure (DP) transducer cell (DP cell) to measure the pressure drops experienced along the length of the riser.

1.1. Slug flow characterization

The principal features of slug flow are well explained by the model proposed by Dukler and Hubbard (1975). Their model is based on the observation that the slug behaves as a kinematic wave. Here, a fast moving liquid slug overruns and picks up a slow moving liquid film in front of it. The liquid scooping mechanism is due to the pressure drop that occurs during the acceleration of the liquid from the liquid layer by the front of the liquid slug body, Fig. 1. The kinematic wave velocity is actually higher than the actual velocity of the liquid particles inside the liquid slug body. Therefore, using a reference frame that moves at the wave velocity, the liquid moves across the liquid slug body. From a stationary reference frame, the liquid velocity decreases due to friction. The force due to the frictional pressure drop is the mechanism for the liquid shedding from the tail of the liquid slug body.

This Hubbard and Dukler (1975) model serves as a basic reference to the hydrodynamic behaviour of the slug flow pattern. A brief synopsis of the different methods to determine the characteristics of slug flow is presented, below:

1.1.1. Slug velocity

The slug front translational velocity, U_T, is often approximated using the approach known as the drift flux model, also suggested by Nicholson et al. (1978).

$$U_T = 1.2U_S + U_D \tag{1}$$

Where, U_s is the average velocity of the liquid in the slug. For homogeneous, no-slip flow in the slug body, $U_s = U_M$. Where U_M is the mixture superficial velocity. Therefore, the term $1.2U_M$ is approximately equal to the maximum velocity that the liquid in the slug may achieve. The drift velocity, U_D, in Eq. (1) is the relative velocity between U_T, and the maximum velocity of the liquid in the slug, $1.2U_s$.

As reported in the literature, the drift velocity is clearly non-zero for inclined flows. Early works of Hubbard and Dukler (1966), Gregory and Scott (1969), as well as Heywood and Richardson (1979), proposed that the drift velocity, $U_D = 0$, for horizontal flows. In contrast, later other investigators, such as, Nicholson et al. (1978), and Kouba (1986), have noted significant drift velocities in horizontal pipes.

Davies and Taylor (1950) show that, the bubble drift velocity in vertical tube is:

$$U_{D_{vertical}} = 0.35\sqrt{gD} \tag{2}$$

For horizontal pipes, Benjamin (1968) proposes the following relation:

$$U_{D_{horizontal}} = 0.54\sqrt{gD} \tag{3}$$

Where, g and D are acceleration due to gravity and pipe internal diameter, respectively.

1.1.2. Liquid holdup in the liquid slug body

One of the primary variables required to characterize slug flows is the liquid holdup in the slug body, H_s. Table 1 presents a summary of the slug body liquid holdup models considered by this study.

1.1.3. Slug length

The determination of the slug length (or frequency) is a key characterization parameter within almost all of the proposed slug flow models. According to Hernandez-Perez (2008), the prediction of the slug length is perhaps the most difficult parameter to estimate. Slug length has been found to be strongly dependent on the diameter of the carrier pipeline. This can complicate the application of correlation models obtained on small diameter test facilities to scale-up of larger field scale facilities.

A series of investigators Taitel and Dukler (1977), Nydal et al. (1991) and Barnea and Taitel (1993), report stable slug lengths of 15–40 pipe diameters in horizontal and slightly inclined pipes. All of these studies concluded that the slug length is fairly insensitive to the gas and liquid flow rates, and depend principally on the pipe diameter.

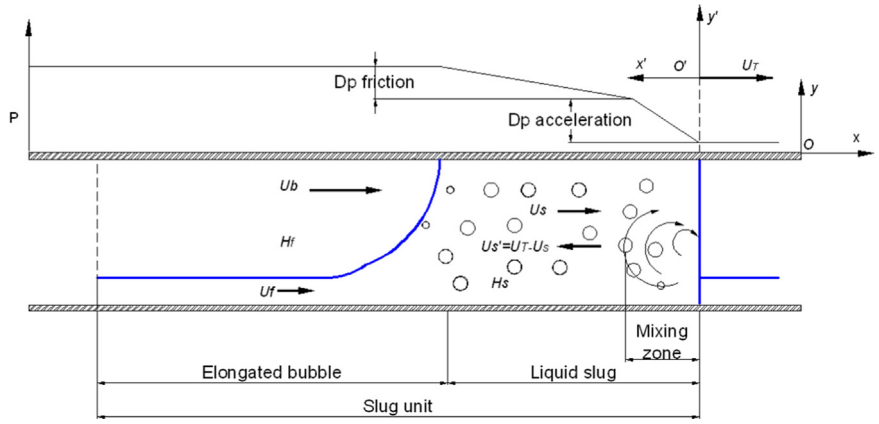

Fig. 1. Schematic representation of the Dukler and Hubbard (1975) slug flow model. Where, U_f, U_s, U_s' are the average liquid velocity in the film, average velocity of the liquid in the slug, difference between the slug front velocity and average velocity of the liquid in the slug, respectively. $U_b = U_T$, represents the slug front velocity, Hs and Hf are the liquid holdups in the liquid slug and liquid film, respectively. Dp is pressure difference.

Table 1
Summary of slug body liquid holdup correlations. Where, σ, ρ_L, μ_L, Re_L, and θ are the surface tension, liquid density, liquid viscosity, slug Reynolds number and pipe angle, respectively.

Model	Pipe internal diameter (mm)	FLUID	Liquid holdup in the liquid slug body	
Gregory et al. (1978)	25.8, 51.2	Air/Light Oil	$H_s = \frac{1}{1 + \left(\frac{U_M}{8.66}\right)^{1.39}}$	(4)
Malnes (1983)	25.8, 51.2	Air/Light Oil	$H_s = 1 - \frac{U_M}{\left[83\left(\frac{g\sigma}{\rho_L}\right)^{1/4} + U_M\right]}$	(5)
Marcano et al. (1998)	78	Air/Kerosene	$H_s = \frac{1}{1.001 + 0.0179U_M + 0.0011U_M^2}$	(6)
Gomez et al. (2000)	51 to 203	Air/Water Air/Oil	$H_s = e^{-(0.45\theta + C\mathrm{Re}_L)}$, $0 \le \theta \le \frac{\pi}{2}$	(7)
		Freon/Water	$C = 2.48 \times 10^{-6}$; $\mathrm{Re}_L = \frac{\rho_L U_M D}{\mu_L}$	(8)

Table 2
Summary of fully developed slug frequency models. Where, U_{SL} is liquid superficial velocity.

Model	Pipe internal diameter (mm)	Fluid	Slug frequency	
Heywood and Richardson(1979)	42	Air–Water	$f_s = 0.0434\left[\frac{U_{SL}}{U_M}\left(\frac{2.02}{D} + \frac{U_M^2}{gD}\right)\right]^{1.02}$	(9)
Hubbard (1965)	19	CO_2–Water	$f_s = 0.0226\left[\frac{U_{SL}}{gD}\left(\frac{19.75}{U_M} + U_M\right)\right]^{1.2}$	(10)
Nydal et al. (1991)	52.9 and 90	Air–Water	$f_s = \frac{0.088}{gD}(U_{SL} + 1.5)^2$	(11)
Greskovich and Shrier (1972)	45	CO_2–Water	$f_s = 0.0226\left[\frac{U_{SL}}{gD}\left(\frac{2.02}{D} + \frac{U_M^2}{gD}\right)\right]^{1.2}$	(12)
Jepson and Taylor (1993)	306	Air–Water	$f_s = \frac{U_{SL}}{D}(0.00759U_M + 0.01)$	(13)
Zabaras (1999)	25 to 203	Air–Water Air–Oil	$f_s = 0.0226\left[\frac{U_{SL}}{gD}\left(\frac{19.75}{U_M} + U_M\right)\right]^{1.2}[0.836 + 2.75Sin\theta]$	(14)

1.1.4. Slug frequency

Gregory and Scott (1969) define the slug frequency, f_s as the average number of slug units passing a given point in the system over a unit of time. And despite the availability of the many slug frequency data sets reported in the literature, it is still considered the least reliably estimated parameter, due to the stochastic nature of slug flow patterns and the intermittency of the flows. However, due to its inclusion as a closure relation in many slug flow models, it is important to accurately predict this parameter. The variation in slug frequency observed depends on whether if the flow is developing or fully developed.

Table 2 presents a summary of the slug frequency models considered by this study.

It is clear from the analysis and discussion of the experimental data of the gas–liquid studies presented above that there are many parameters that influence the hydrodynamic behaviour of slug flow. Some of these are the fluid properties. To investigate the characteristics that may result using relevant fluids; experiments were conducted using ECT and DP cell to enable detailed characterization of the observed air and silicone oil slug flows in a

horizontal pipe. This was achieved by the measurement of the instantaneous distribution of the transient flow phases observed over the surveyed cross-sections of the pipe. The use of two sets of circumferential ring sensor ECT electrodes, located 89 mm apart, enabled the determination of the slug translational velocities of the observed elongated bubbles and liquid slugs as they passed through the surveyed cross sections. Also determined are the slug frequencies, lengths of the elongated bubbles and liquid slugs, and void fractions in the elongated bubble and liquid slug. A DP cell was used to measure the pressure drops experienced along the length of the pipe.

2. Experimental facility

The experiments described in this paper were carried out on an inclinable pipe flow rig within the Chemical Engineering Laboratories at the University of Nottingham. Fig. 2 shows a schematic diagram of this experimental facility. The rig has been employed for a series of earlier published two-phase flow studies, Azzopardi (1997), Hernandez-Perez et al. (2010), Abdulkadir et al. (2011), Abdulkadir et al. (2014), and Abdulkadir et al. (2015). The horizontal experimental pipe test section of the facility consists of a 6 m length, 0.067 m internal diameter transparent acrylic pipe which allows for the visualization and measurement of the development of the

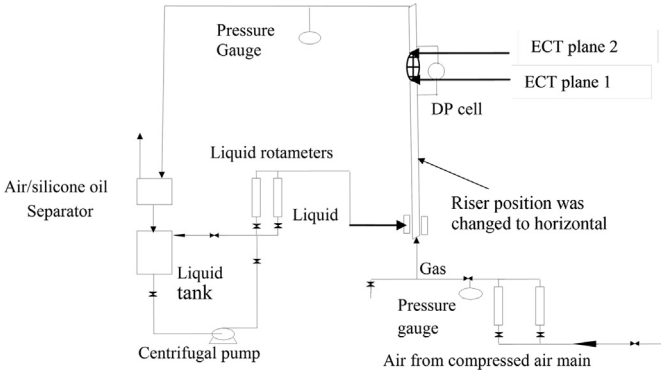

Fig. 2. A schematic diagram of the experimental riser rig inclined to be become a horizontal pipe as shown in Fig. 3. The physical measurements recorded on this rig were used to determine parameters that could subsequently be used to characterize the flow regime observed within the horizontal pipe section when the flow rates of both the silicone oil and the air streams were varied, Abdulkadir et al. (2014).

injected flows across the length of the test section. The test pipe section may be rotated on the rig to allow it to lie at any inclination angle of between -5 to 90° to the horizontal. For the experiments reported in this paper the rig test pipe section was mounted as a horizontal pipe (an inclination of 0° to the horizontal) as shown in Fig. 3. Great care was taken to ensure that the pipe was true horizontal using a level tool and by adjusting the winch.

The rig was charged with an air–silicone oil mixture to study the flow regimes created. The experiments were all performed at an ambient laboratory temperature of approximately 20 °C. The resultant flow patterns created across the range of air injection–silicone oil circulation flow rates studied were measured using twin-plane ECT transducer. The measurements were made at an acquisition frequency of 200 Hz over a period of 60 s for each experimental flow run. In this study, a ring of electrodes was placed around the circumference of the horizontal pipe at a given distance from the inlet of the 6 m horizontal pipe section. This enabled the measurement of the instantaneous distribution of the flow phases over the cross-section of the pipe. The use of two such circumferential rings of sensor electrodes, located at a specified distance apart (also known as twin-plane sensors), enabled the determination of the translational velocity of any observed elongated bubbles and associated liquid slugs. The twin-plane ECT sensors were placed at distances of 4.4 and 4.489 m upstream of the air–silicone oil mixer injection portal located at the base of the horizontal pipe. A more detailed technical description may be found in Abdulkadir et al. (2014).

In order to measure the pressure drop, a DP cell (Rosemount 1151 smart model) with a range of 0–37.4 kPa, and an output voltage of 1–5 V, was mounted on the pipe to record the pressure drop along the horizontal pipe flow test section. The exact axial locations of the tappings are 4.5 m and 5.36 m (67 and 80 pipe diameters, respectively) from the inlet of the test pipe flow section. Thus, the pressure drop using DP cell was measured simultaneously together with void fraction using the ECTs. The output of the DP cell was recorded to a computer hard disk using the LABVIEW 7 software (National Instruments), and was taken at a sampling frequency of 1000 Hz over 60 s for each flow run experiment.

Each experiment was repeated twice to estimate measurement repeatability. The average standard deviation of the data recorded was ±2%.

The physical properties of the air–silicone oil system and the values of the dimensionless numbers, Eo, N_f and Mo are presented in Table 3. The measurement uncertainties determined are presented in Table 4.

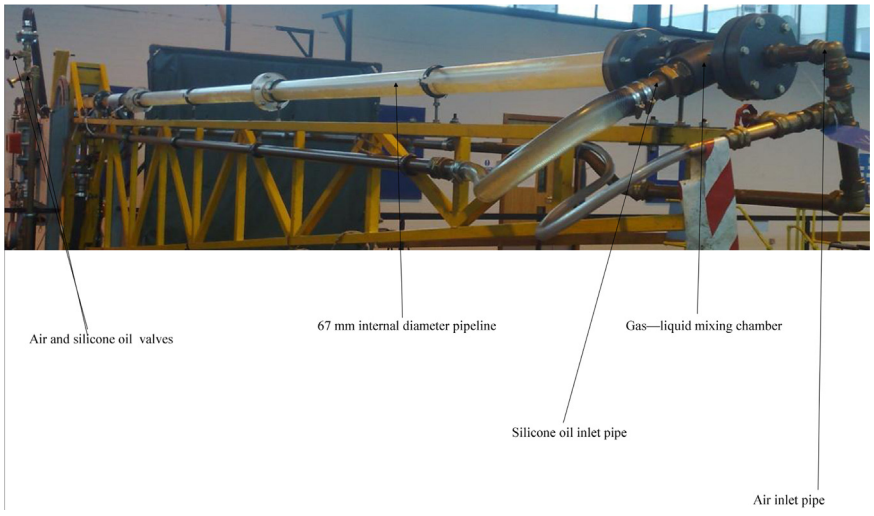

Fig. 3. Picture of the experimental rig in this study.

Table 3
Properties of the fluids and dimensionless numbers at 1 bar and at the operating temperature of 20 °C.

Fluid	Density (kg m^{-3})	Viscosity (kg m^{-1} s^{-1})	Surface tension (N m^{-1})
Air	1.18	0.000018	
Silicone oil	900	0.0053	0.02
Dimensionless numbers			
Eotvos number	Eo = 1981.67		
Dimensionless inverse viscosity	N_f = 9311.72		
Morton's number	$Mo = 1.035 \times 10^{-6}$		

Table 4
Measurement uncertainties.

Measurement	Uncertainty range
Temperature (°C)	±0.5
Liquid superficial velocity (m s^{-1})	±10%
Gas superficial velocity (m s^{-1})	±0.5 – 5%
Void fraction	±10% of the reading
Pressure drop	±0.44 of scale

2.1. Gas-liquid mixing section

The mixing device used in this work is made from Polyvinyl chloride (PVC) pipe as shown in Fig. 4. The silicone oil enters the mixing chamber from one side and flows around a perforated cylinder through which the air is introduced from the bottom of the mixing chamber directly into the two-phase stream through a porous wall section which has 100 holes of 3 mm internal diameter. This arrangement ensures that the gas and liquid flows were well mixed at the entry to the test section. The inlet volumetric flow rates of the liquid and air were determined by a set of rotameters located above a set of valves on the two inlets feed flow pipes.

3. Results and discussion

Khatib and Richardson (1984) and Costigan and Whalley (1997), among others, have shown that void fractions that produce a twin peaked probability density function (PDF) represent slug flows, as shown in Fig. 5. They further highlighted that low void fraction of the PDF peak corresponds to a liquid slug, whilst the high void fraction peak represents an elongated bubble. Employing this concept to interpret the PDFs of the recorded void fractions, it is determined that slug flows are created within the horizontal pipe for liquid superficial velocities of between 0.05–0.47 m s^{-1} and gas superficial velocities of between 0.29–1.42 m s^{-1}. This is also in agreement with a plot of these data points on a Shoham (2006) flow pattern map, Fig. 6.

The PDF as described by Abdulkadir et al. (2014), was created by counting the number of data points in bins of width 0.01 centred on void fractions from 0.005, 0.015…0.0.995, and then dividing each sum by the total number of data points. This method identifies the dominant void fractions which are observed at each flow condition.

An analysis of the recorded time series of void fraction enables the determination of the: slug translational velocity, slug frequency, lengths of liquid slug, elongated bubble and slug unit, void fraction within the liquid slug and elongated bubble.

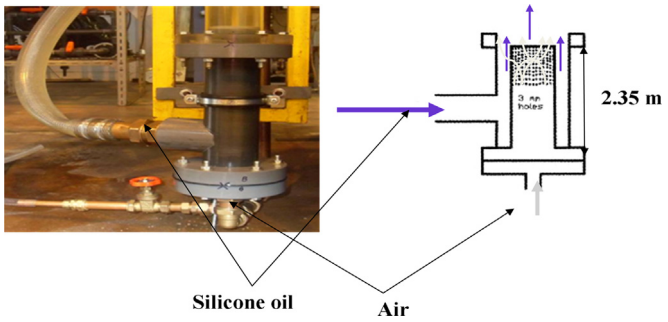

Fig. 4. Air–silicone oil mixing section, Abdulkadir et al. (2014).

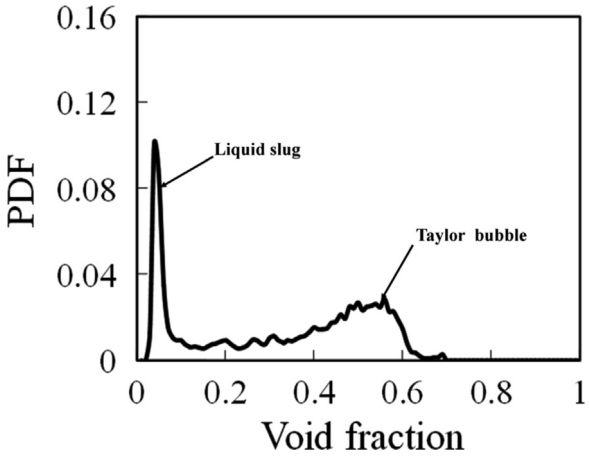

Fig. 5. A typical PDF of void fraction. Liquid superficial velocity = 0.19 m s^{-1} and gas superficial velocity = 0.95 m s^{-1}.

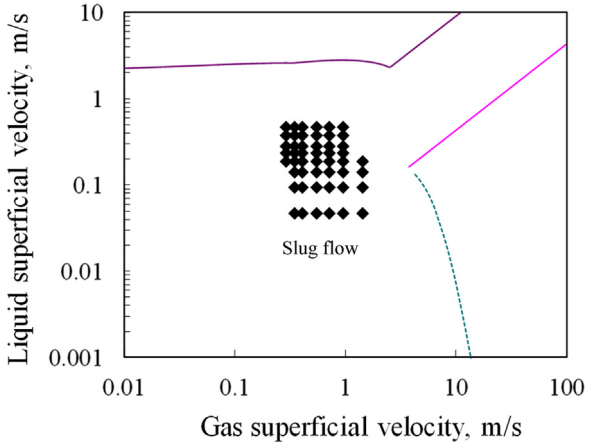

Fig. 6. A plot of the experimental data points on a Shoham (2006) flow pattern map, which confirms that all of the plotted experimental conditions lie within the slug flow region.

3.1. Validation (Testing) of ECT Data

In this study, the ECT measurement transducers were used to give detailed information about air–silicone oil flows, whilst the wire mesh sensor (WMS), installed downstream of the ECT flow measurement section, provides a check on the void fraction measurement accuracy. A detailed description of WMS technology is provided by da Silva et al. (2010). The capacitance WMS, placed at 4.92 m away from the mixing section (73 pipe diameters) was used to image the dielectric components in the pipe flow phases by measuring rapidly and continually the capacitances of the

passing flow across several crossing points in the mesh.

Experimental measurements were recorded with the aid of the above instrumentation across a range of liquid superficial velocities and air superficial velocities of between 0.05–0.47 m s^{-1} and 0.05–4.73 m s^{-1}, respectively. The flow patterns observed across these liquid and gas superficial velocities include: bubble, plug, slug and stratified wavy flows. The measurement sequence was programmed to allow simultaneous measurements and recordings from the WMS and ECT transducers, Abdulkadir et al. (2014). The sampling frequencies of the ECT and WMS measurement transducers were 200 and 1,000 Hz, respectively. Fig. 7 shows a comparative plot of average void fractions recorded by the ECT and WMS measurement transducers. The data presented on the figure illustrates good agreement between the two measurements techniques. Abdulkadir et al. (2014) suggest that some of the minor differences may be due to the fact that the ECTs take measurements over larger axial distances than the WMS.

3.2. Flow development

To investigate the influence of pipeline length on slug flow, the void fractions determined from the measurements recorded by two ECT probes and a WMS transducer located as shown in Fig. 8, along the horizontal test pipe section were examined to resolve the flow development. A fully developed flow is one where the observed flow pattern does not change with the distance downstream, Abdulkadir et al. (2012). To interrogate such a flow development, the obtained average slug frequency and the PDFs of the void fractions are presented as a function of the distance on Fig. 9 and Table 5, respectively.

The average slug frequencies and the PDFs of the void fractions are determined for three cross-sections along the length of the horizontal pipe length (at distances of 4400 mm (64 pipe diameter), 4489 mm (67 pipe diameter) and 4920 mm (73.4 pipe diameter) downstream of the gas–liquid mixing section. These correspond to the location of the two ECT–planes and the single WMS measurement transducers, respectively, as shown in Fig. 8. The average slug frequencies and PDFs of void fraction determined from the ECT and WMS measurements are used to identify any changes in flow characteristic along the length of the pipe.

3.2.1. Comparison of slug frequencies against axial distance

An analysis of a plot of the measured average slug frequencies against axial distance, shown in Fig. 9, establishes that there is no significant difference in flow development observed across each of the three mesurement transducer locations, and therefore the flow can be considered to be fully developed at a distance of 4400 mm. This conclusion supports the previous findings of Abdulkadir et al. (2012) which determined that the variations in void fraction recorded at distances of 64, 65, and 66.65 pipe diameters downstream of the mixer were small, and concluded that the flow is fully developed at 64 pipe diameters. These findings also agree with Weisman et al. (1979) and Woods and Hanratty (2006) who confirm that for a simple mixing device, and in the absence of bends, an equilibrium in the pipe flow development is reached at a dimensionlesss distance, L/D ≈60, downstream. Any small changes in flow development observed at an axial distance of 4920 mm, may be attributed to the slight disturbance that the more intrusive

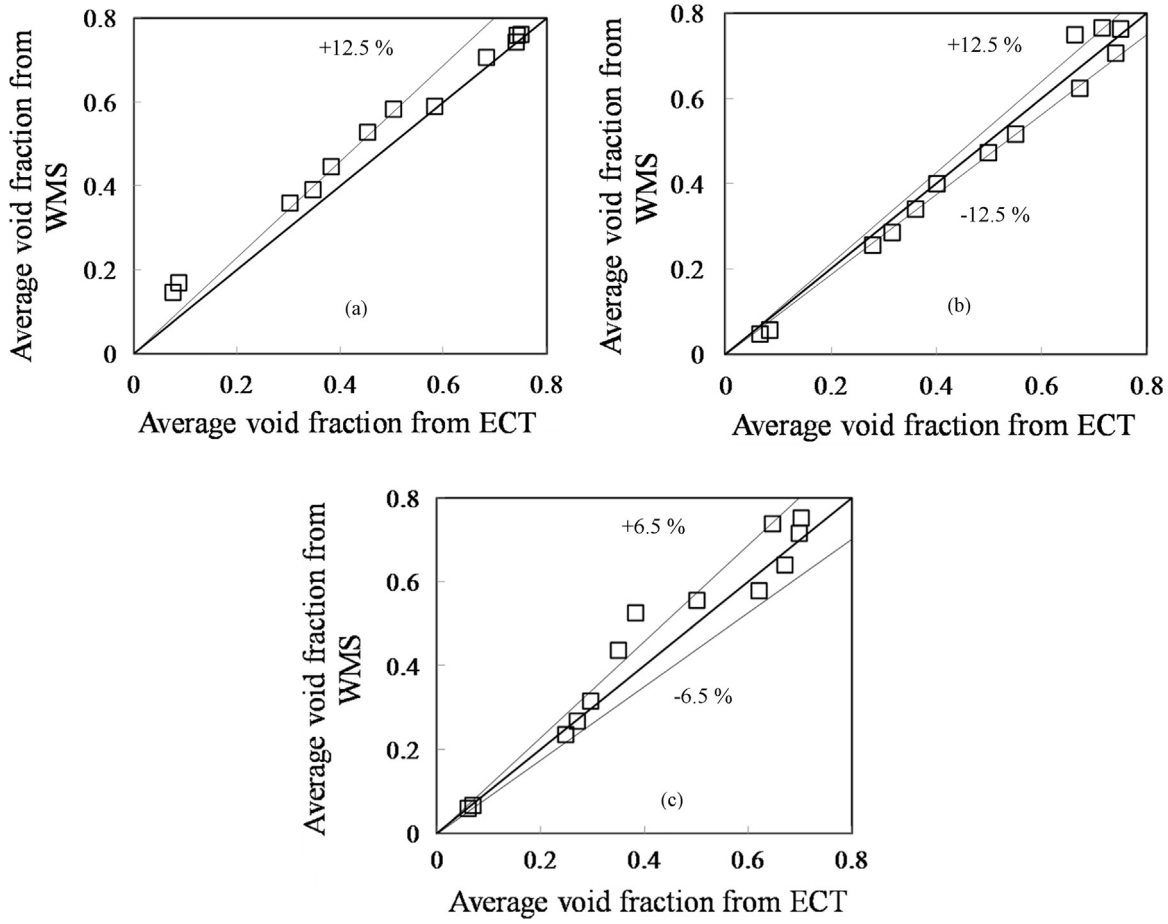

Fig. 7. Comparison of average void fraction obtained from the ECT and WMS (a) Liquid superficial velocity = 0.14 m $s^{-1}$and gas superficial velocity = 0.05 – 4.73 m s^{-1} (b) Liquid superficial velocity = 0.28 m s^{-1} and gas superficial velocity = 0.05 – 4.73 m s^{-1} (c) Liquid superficial velocity = 0.38 m s^{-1} and gas superficial velocity = 0.05 – 4.73 m s^{-1}.

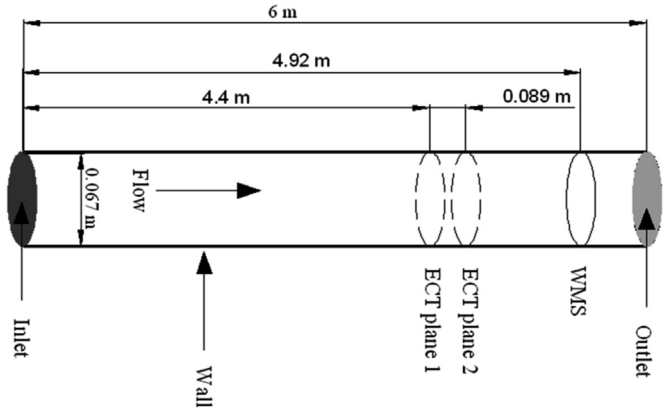

Fig. 8. Horizontal pipe used in this study showing measurement locations.

WMS transducer may introduce to the flow.

An examination of the form of the determined PDF of void fraction shown on Table 5 concludes that the observed flow patterns are slug flows, characterized by a double peak trace, the lower peak representing the liquid slug and the higher peak representing the elongated bubble.

3.2.2. Comparison of slug front and slug tail

Another way to confirm flow development is to compare the slug front and tail velocities. Developing slugs may be characterized by the determination of the slug front and the bubble front velocities. The slug front and tail velocities, U_f and U_t, respectively, are calculated by the determination of the arrival times of the slug front and tail at two adjacent planes, and then dividing the distance, Δx, between them by the respective time differences, Δt.

A comparison of the slug front and tail velocities can provide a better indicator of flow development, as a growing slug might have different front and tail velocities. A computer code was written to calculate slug front and tail velocities from the measured values. The computer algorithm identifies the time delay between signals recorded by the two plane ECTs, when the liquid holdup within the measured flow is in the range of between 60–80%. This is numerically established by computing the intersection point between the liquid holdup signal and a horizontal line. Further modifications were required to make the algorithm more robust, to deal with any irregularities of flow observed. From an analysis of the plotted experimental results presented on Fig. 10, we can see that the differences between the measured slug front and tail velocities are small for the majority of the flow conditions considered, which indicates good flow development. This finding is in agreement with Ujang et al. (2006), who reported frequency at different lengths, where flow development seems to be affected by the liquid superficial velocity. An examination of their results suggests that a liquid superficial velocity of around 0.8–1.0 m s^{-1} would be required for the development length to be more than 5 m in our pipe.

The present results show the flow characteristics within a limited distance (6 m in length) in which the outlet pressure is near atmospheric. When the pipe is much longer, due to pressure drop, the gas will expand, increasing the local volumetric flow rate. As a result, the insitu gas superficial velocity will increase. In the flow pattern map, this suggests that a change in the insitu flow pattern would occur from slug to wavy and annular flow. From a phenomenological point of view, using the model of Dukler and Hubbard (1975), the gas expansion will lead to an increase in the large bubble nose velocity, increasing the shedding of liquid at the tail of the liquid slug. Since the scooping of liquid at the liquid slug front remains constant, the liquid slug length will decrease, turning into pseudo slugs and then waves. If the outlet pressure is kept constant, for the longer pipe, a higher inlet pressure would be required to drive the flow through. For an infinitely long pipe, this is expected to happen indefinitely. This argument suggests that, completely steady slug flow may never be achieved. Sakaguchi et al. (1987) much later experimentally studied the dynamic behaviours of the transient slug flow and of its impact force using air–water two-phase flow in a horizontal pipe. They theoretically analyzed the phenomena of the transient slug flow by applying the scooping-shedding model and generalized integral balances of mass and momentum. They concluded that the phenomena unanticipated from the steady flow condition occur under the transient flow condition, and that the large impact force is caused by a rapid ejection of the transient liquid slug.

3.3. Determination of characterization parameters

3.3.1. Slug translational velocity

Cross-correlation of the time series of void fraction determined from the measurements recorded at the two ECT probes allows the slug translational velocities of periodical structures such as slugs to be determined. A plot of the time series of the void fractions recorded by the two ECT probes is shown in Fig. 11. The details of the cross-correlation method used may be found in Abdulkadir et al. (2014). The slug translational velocities calculated for all of the experiments performed are presented in Fig. 12.

Fig. 12a shows a plot of the determined slug translational velocities values. It can be observed that for a given liquid superficial velocity, the slug translational velocity is observed to increase as the gas superficial velocity increases.

Using the drift-flux approach, Bendiksen (1984) expressed the

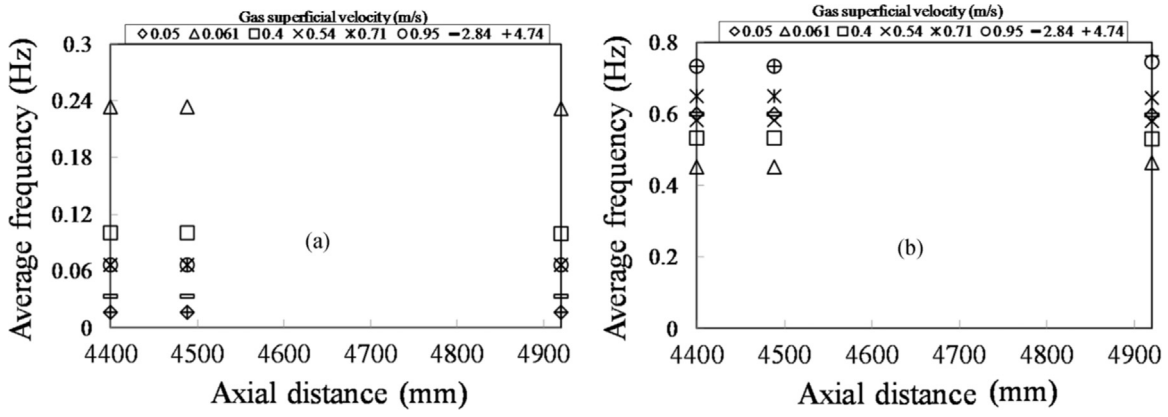

Fig. 9. A plot of the average measured slug frequencies against the axial distance downstream of the gas-liquid mixing section for the liquid superficial velocities of: (a) 0.05 and (b) 0.38 m s^{-1}.

Table 5
A plot of the PDFs determined for the void fractions measured at the three transducer locations along the length of the horizontal pipe downstream of the gas–liquid mixing section.

Flow condition		Measuring station (mm)		
U_{SL} (m s^{-1})	U_{SG} (m s^{-1})	4400	4489	4920
0.05	0.40	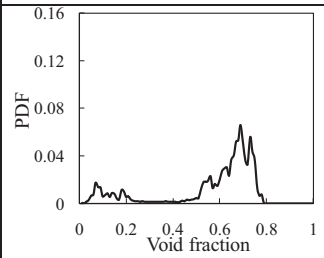	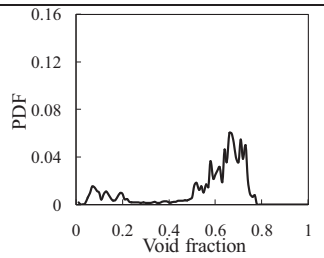	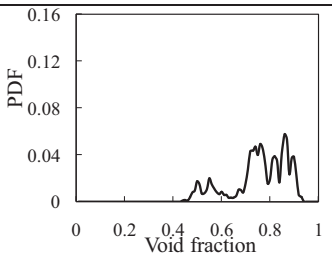
0.38	0.40	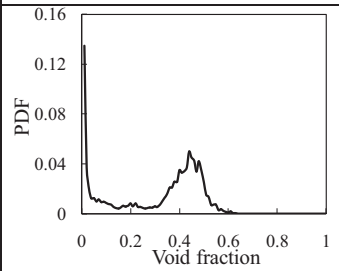	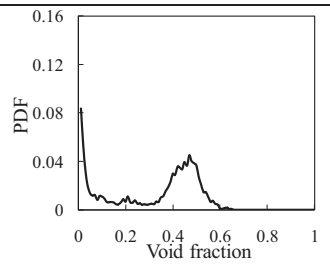	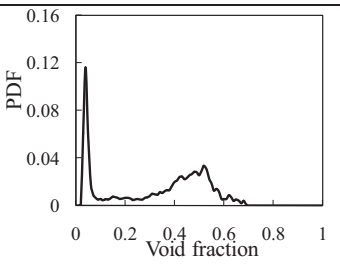
0.47	0.40	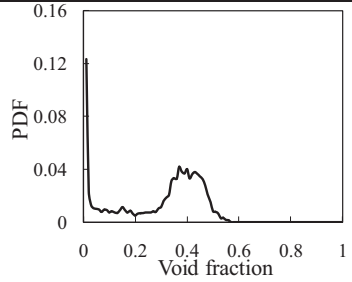	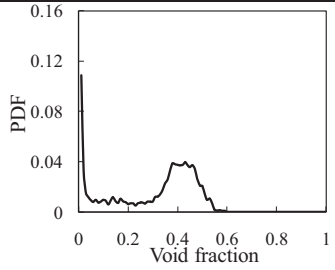	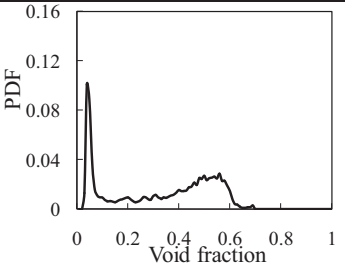

slug translational velocity as a linear function of mixture superficial velocity (U_M) and drift velocity (U_D), such that

$$V_T = C_o U_M + U_D \tag{15}$$

Considering a wide range of slug flow conditions, Zheng et al. (1994) experimentally obtained a value of 1.20 for C_o. The drift velocity U_D, according to Benjamin (1968), is due to gravity current effects, and is also reported to be dependent on pipe internal diameter, phase distributions and to the local slip resulting from the lateral and axial pressure gradients. According to Franca and Lahey (1992), the slug translational velocities in the small diameter pipe would be slightly smaller than those observed in the larger pipe. It is worthwhile noticing that if the slug translational velocity data of Weber (1981), Bendiksen (1984) (19–50 mm internal diameter, air–water system) and present data (67 mm internal diameter, air–silicone oil) is presented in Fig. 12b, the slope C_o and the intercept U_D are found to be 1.239 and 0.446, respectively. Thus, the correlating line of the graph has the relationship

$$U_T = 1.239U_M + 0.446 = 1.239U_M + 0.55\sqrt{gD}. \tag{16}$$

It is reported in the literature that the value of the coefficient C_o can vary between values of 1.2-1.35. Abdulkadir et al. (2014) reports $C_o = 1.39$ for a vertical pipe using air–silicone oil mixture as the operating fluid. In Fig. 12, the observed non-zero intercept of the line with the y-axis shows that there is a drift velocity component associated with the bubbles. This result supports the conclusions of Nicholson et al. (1978), Weber (1981) and Bendiksen (1984) that a drift velocity exists for the horizontal case and that it may even exceed its value in the vertical case.

The ratio of the slug translational velocity to mixture superficial velocity, U_T/U_M is plotted against gas superficial velocity in Fig. 13. The plot shows that at liquid and gas superficial velocities of 0.05 and 0.34 m s^{-1}, respectively, $U_T/U_M = 2.1$. However, as the gas superficial velocity is gradually increased, U_T/U_M monotonically decreases from a value of 2.1-1.3. These observations are consistent with the conclusions of Jepson and Taylor (1993). It may be concluded that for the eight liquid superficial velocities considered here that the value of U_T/U_M is between 2.3 and 1.3 and is observed to decrease as the gas superficial velocity increases. Crowley et al. (1984) report values of $U_T/U_M = 2.0$–1.35 for slug flow in a 0.17 m internal diameter pipe and that the values are dependent on fluid properties.

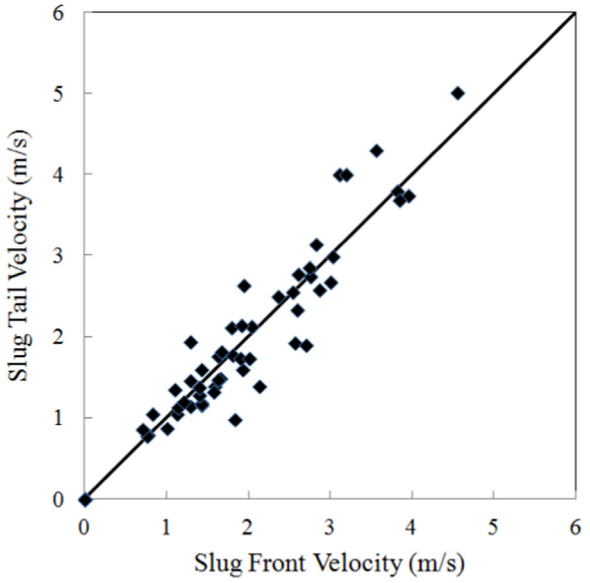

Fig. 10. A comparison between the slug front and tail velocities determined for a range of different gas and liquid superficial velocities.

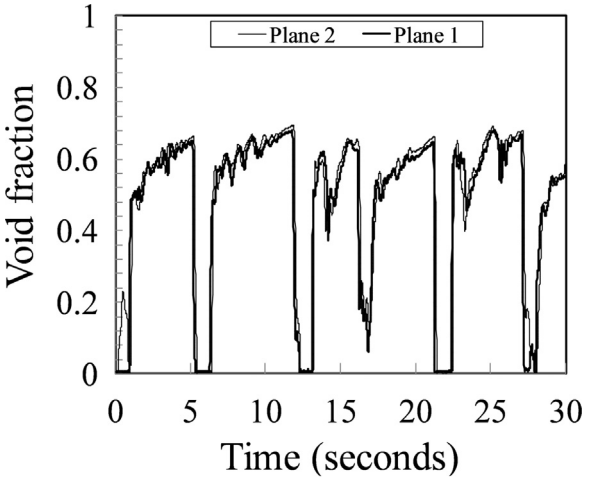

Fig. 11. A typical plot of the void fraction signals recorded from the two ECT probes. The distance between the two ECT probes is 89 mm. The liquid and gas superficial velocities are 0.05 m s^{-1} and 0.34 m s^{-1}, respectively.

3.3.2. Pressure gradient

Fig. 14 presents a plot of the frictional pressure gradient measured as the gas superficial velocity is increased, for a range of increasing liquid superficial velocities. The plot shows that in general the frictional pressure gradient increases with gas superficial velocity. In general, the observed increase in frictional pressure gradient can be attributed to an increase in shear stress between the liquid and the walls of the pipe and comparatively larger bubbles are observed to form due to coalescence, which causes a decrease in the liquid velocity due to higher level of liquid holdup, hence an increase in the frictional pressure drop. These observations support the phenomena reported by Beggs and Brill (1973) and Barnea and Brauner (1985). However, the observed decrease on the other hand could be attributed to the fact that the slugs are completely frothy and as a consequence results in a decrease in frictional pressure gradient as the gas superficial velocity increases. A similar observation is reported by Jepson and Taylor (1993).

3.3.3. Average cross-sectional void fraction

Fig. 15 shows that the average void fraction determined across the range of Eotvos number is $0.23 \leq \bar{\varepsilon} \leq 0.78$. It is evident that, in general, the average void fraction increases with an increase in gas superficial velocity at constant liquid superficial velocity. However, at liquid superficial velocity of 0.05 m s^{-1}, small fluctuations happen, which could be attributed to bubble collapse and air entrainment in the liquid layer as a result of an increase in the gas superficial velocity.

3.3.4. Void fraction in the liquid slug and elongated bubble

In the present work, regular slugs are identified using the PDF of void fraction forms suggested by Nydal et al. (1991). PDF functions are bimodal for slug flow illustrated in Fig. 5. Here, the PDF of void fraction shows two main peaks, a low and high void fraction corresponding to 0.06 and 0.72, respectively. These peaks are the signatures of the aerated liquid slug and the elongated bubble.

The average void fraction in the liquid slugs is presented in Fig. 16. These values are of regular slugs. It can be observed that for these conditions void fraction is almost insensitive to both the liquid and gas superficial velocities. This is in agreement with the findings of Dukler and Hubbard (1975), Barnea and Brauner (1985) and Nydal et al. (1991).

Fig. 17 presents a plot of the void fraction in the elongated bubble against the gas superficial velocity. It is observed that, as expected, the void fraction in the elongated bubble increases as the gas velocity increases. At liquid superficial velocities of between 0.14–0.47 m s^{-1}, an exponential relationship is established between the void fraction in the elongated bubble and the gas superficial velocity.

Fig. 18 presents a relation of the void fraction in the elongated bubble (ε_{EB}) to the void fraction in the slug body (ε_S). Interestingly, ε_{EB} is observed to have a maximum value of 0.8 with an increase in ε_S. For the case of $\varepsilon_S = 0.01$, the liquid slug may be classified as a homogeneous bubble flow, whilst on the other hand, the liquid slug may be regarded as the development of a discrete bubble in the region $0.01 < \varepsilon_S < 0.15$.

3.3.5. Slug length

Fig. 19, illustrates the ratio of length of liquid slug to length of elongated bubble (L_S/L_{EB}) as a function of gas superficial velocity over a range of different liquid superficial velocities. It is observed that, as expected, L_S/L_{EB} is observed to decrease with an increase in gas superficial velocity. Contrary to this, at liquid superficial velocity of 0.05 m s^{-1}, L_S/L_{EB} is almost independent of the gas superficial velocity. L_S/L_{EB} seems to approach zero as gas superficial velocity gets bigger. For the parameter values below the dash line, as depicted in Fig. 18, the length of the elongated bubble is bigger than liquid slug, whilst on the other hand, the liquid slug is longer for the region above the dash line.

The slug unit length (L_U), which is defined as the sum of slug and elongated bubble (liquid film) lengths

$$L_U = L_S + L_{EB} \tag{17}$$

is determined by multiplying the translational elongated bubble velocity by the time taken for the slug unit to travel the distance between the two ECT probes. Thus, the length of a slug unit is given by

$$L_U = \frac{U_T}{f_s} \tag{18}$$

Fig. 20 illustrates a plot of the measured average dimensionless slug unit length against the gas superficial velocity. These lengths were determined over an average experimental measurement

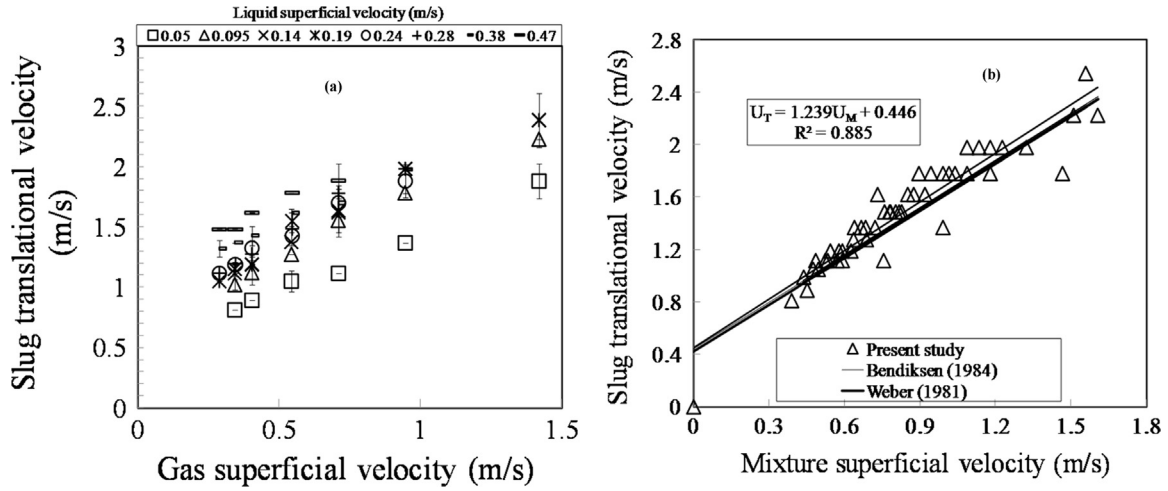

Fig. 12. (a) A plot of the experimentally determined slug translational velocity (structure velocity) as a function of mixture superficial velocity for a set of flow data corresponding to a slug flow pattern. (b) A comparative plot of the determined slug translational velocities measured from experiment and those determined from empirical correlations. The empirical equations used are those proposed by Weber (1981) and Bendiksen (1984), which were recalculated using the physical properties of air and silicone oil.

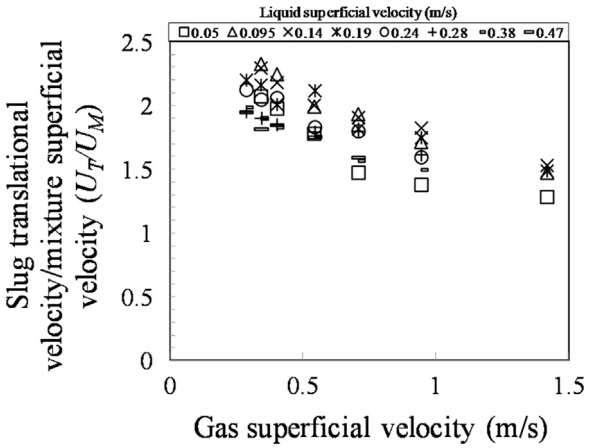

Fig. 13. A plot of the variation of the ratio of slug translational velocity, U_T/U_M with gas superficial velocity across a range of liquid superficial velocities.

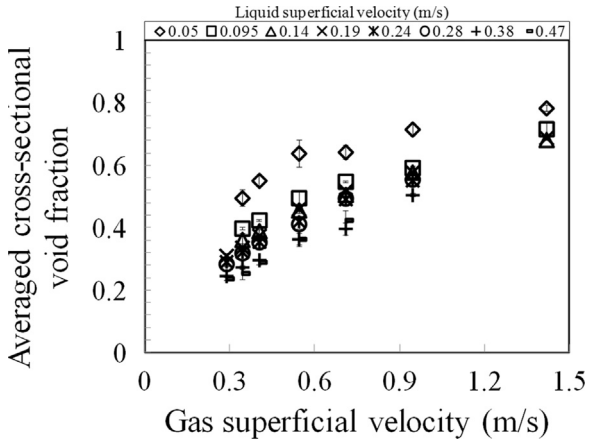

Fig. 15. A plot of experimental data to illustrate the effect of gas superficial velocity on the average cross-sectional void fraction. The bars represent the standard deviation of the measurements.

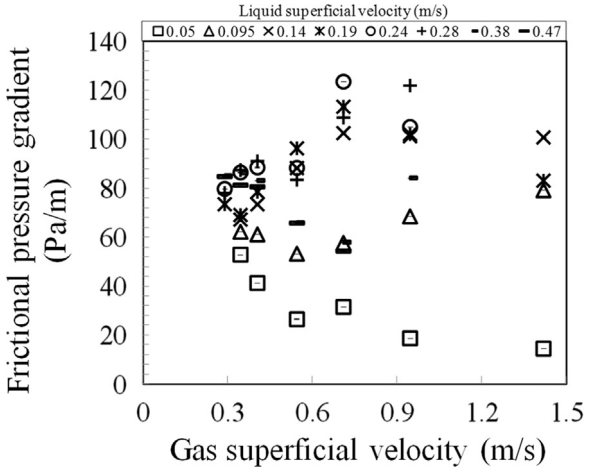

Fig. 14. A plot of the frictional pressure gradient measured as the gas superficial velocity is increased for a range of increasing liquid superficial velocities.

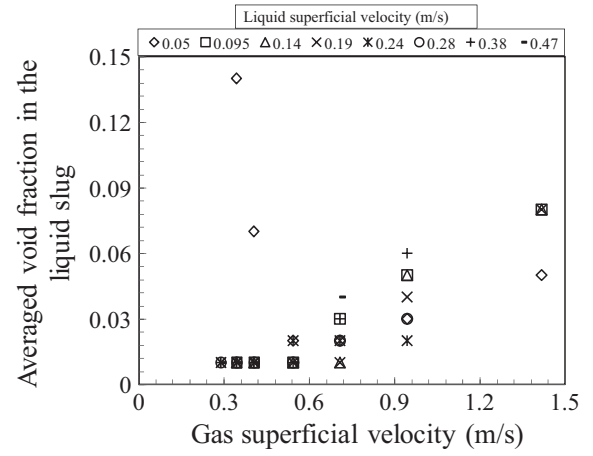

Fig. 16. The determined mean gas void fractions in the liquid slug.

period of 60 s. It can be observed that in general the length of the slug unit increases linearly as the gas superficial velocity increases. For convenience, a dimensionless scaled length is introduced, which is defined as the ratio of length of the observed slug unit divided by the test pipe diameter. It is observed that this length decreases as the liquid superficial velocity is increased from 0.05 to 0.47 m s^{-1} at a gas superficial velocity of 0.54 m s^{-1}. This is to be expected as the frequency of slugging increases as the liquid superficial velocity is increased. A similar observation was

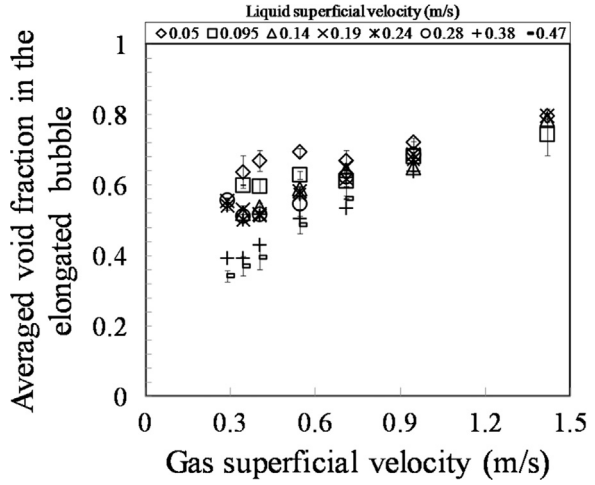

Fig. 17. A plot of the determined mean gas void fractions in the elongated bubbles against the liquid superficial velocities across the range 0.05 – 0.47 m s^{-1}. The bars represent the standard deviation for the plotted experimental measurements.

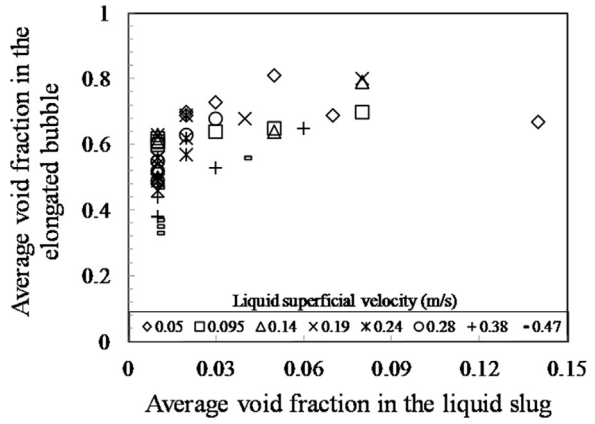

Fig. 18. A plot to illustrate the dependency of the void fraction in the elongated bubble on the void fraction in the liquid slug at different liquid superficial velocities.

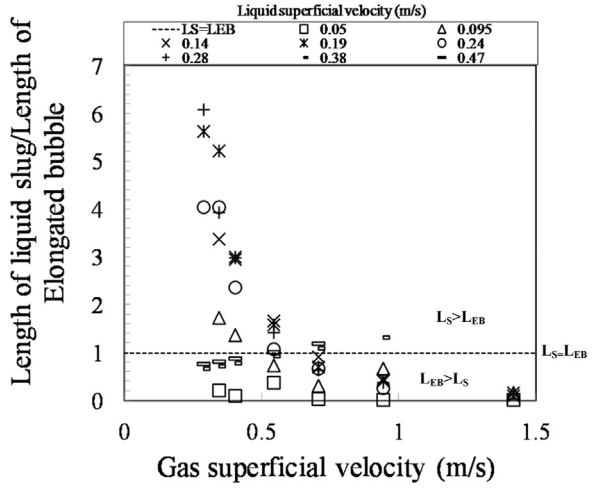

Fig. 19. A plot of the average length of liquid slug/length of elongated bubble (L_S/L_{EB}) as a function of gas superficial velocity across a range of different liquid superficial velocities. Above the dash line, length of liquid slug is bigger than length of elongated bubble. Below the dash line, length of elongated bubble is bigger than length of liquid slug. On the dash line, length of liquid slug is equal to length of elongated bubble.

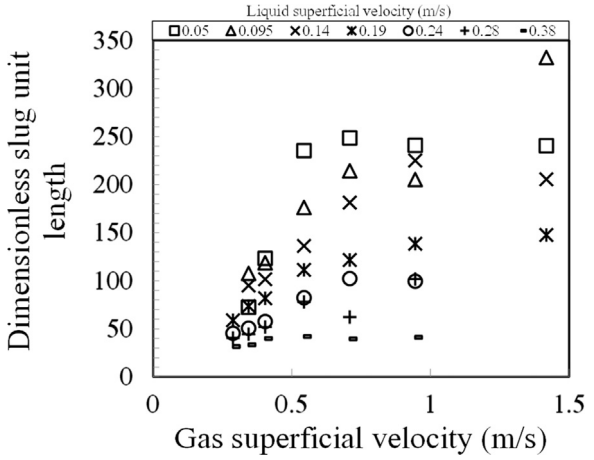

Fig. 20. A plot of the measured dimensionles average slug unit length against the gas superficial velocity. These lengths were determined over an average experimental measurement period of 60 s.

reported by Hernandez-Perez (2008).

By combining the values obtained from Eqs. (17) and (18), the slug and elongated bubble lengths may be determined using the following two expressions:

$$L_S = \frac{L_U}{\frac{L_{EB}}{L_S} + 1} \tag{19}$$

$$L_S = L_U - L_{EB} \tag{20}$$

Fig. 21 illustrates a plot of the average dimensionless liquid slug length against dimensionless unit slug unit length for a range of increasing liquid superficial velocities. An examination of these data trends confirms the characteristic irregularity and intermittency associated with slug flows. A similar trend was reported by Hernandez-Perez (2008). Interestingly, the observed slug lengths are in the order of 8-46 pipe diameters, and appear relatively independent of the flow conditions. A number of other investigators Dukler and Hubbad (1975), Nicholson et al. (1978) and Ferre (1981) observed a fairly constant slug length of between 10 and 40 pipe diameters for a similar set of flow conditions..

Fig. 22 presents a plot of the average dimensionless elongated bubble length against the dimensionless slug unit length for a range of increasing liquid superficial velocities..

It is clear that the elongated bubble length follows a near linear relationship with the total slug unit length. Thus, it may be regarded that the length of the elongated bubble constitutes the main length component of the slug unit.

3.3.6. Frequency

Intermittent flow is characterized by a variation of the observed void fraction with time, mainly in the form of periodic structures. To characterize these structures, an analysis of the fluctuations in void fraction time series was conducted to determine the frequency employing the Power Spectral Density (PSD) method, detailed in Abdulkadir et al. (2014).

Fig. 23 presents a plot of the average slug frequency against liquid superficial velocity for an increasing range of selected gas superficial velocities. It shows that the average slug frequency is fairly weakly dependent on the gas superficial velocity for all of the liquid superficial velocities examined. However, the average slug frequency is clearly observed to increase as the liquid

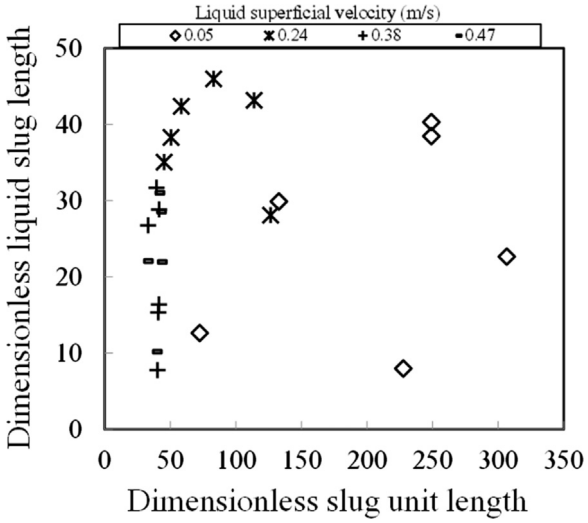

Fig. 21. A plot of the average dimensionless liquid slug length of the dimensionless slug unit length for a range of increasing liquid superficial velocities.

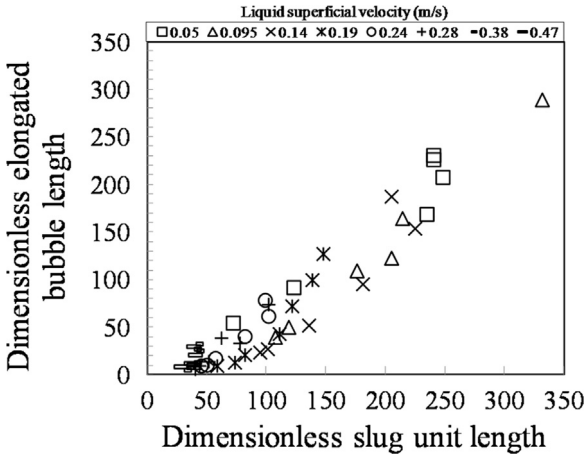

Fig. 22. A plot of the average dimensionless elongated bubble length against the dimensionless slug unit length for a range of increasing liquid superficial velocities.

superficial velocities increase, which confirms the findings of Manolis et al. (1990). This phenomenon may be explained in that the presence of more liquid may be expected to lead to the generation of more slugs as the gas superficial velocity increases.

Comparison of experimentally determined slug frequency against slug frequency obtained from empirical correlations:

Figs. 24 and 25 compare the measured slug frequencies against the empirical equations proposed by Gregory and Scott (1969), Nydal et al. (1991), Jepson and Taylor (1993) and Zabaras (1999). From an examination of these figures it is observed that the predicted values of Nydal et al. (1991) exhibit the greatest discrepancy to the experimental data across all of the liquid superficial velocities considered. The closest agreement between experiment and predicted values is found employing the Zabaras (1999) correlation. The discrepancy with the work of Nydal et al. (1991) may be that this correlation method only considers liquid superficial velocity as a parameter and does not consider the effect of fluid properties and pipe diameter. Thus, the values generated by the empirical methods proposed by Gregory and Scott (1969), Nydal et al. (1991) and Jepson and Taylor (1993) may deviate from the measured experimental values by several orders of magnitude. Thus, in conclusion the correlation method proposed by Zabaras (1999) gave the closest agreement to the current experiment data.

Fig. 26 illustrates a plot of the dimensionless Strouhal number,

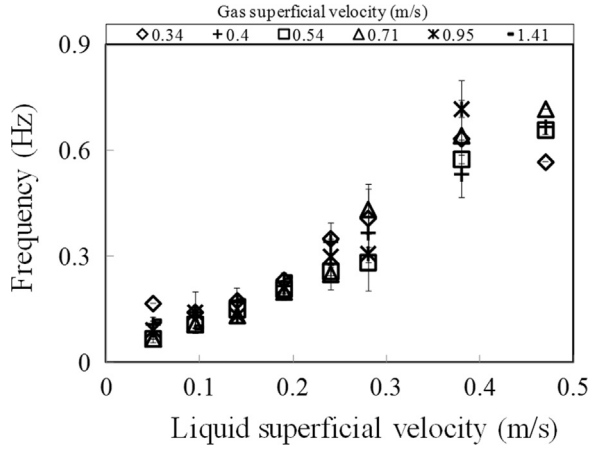

Fig. 23. A plot of the average slug frequency against the liquid superficial velocity for a range of increasing gas superficial velocities. Liquid superficial velocity (m s^{-1}): 0.05 – 0.47. The bars represent the standard deviation for all measurements made.

St, defined as $\frac{f_s D}{U_{SG}}$ as a function of the liquid volume fraction x_L. Where, U_{SG} is the gas superficial velocity. It can be observed from the plot that the experimentally computed *St* values correlate well with those predicted by the model proposed by Fossa et al. (2003) whose constants were inferred from an analysis of the experimental measurements:

$$St = \frac{f_s D}{U_{SG}} = \frac{Ax_L}{1 + Bx_L + Cx_L^2} = \frac{0.044x_L}{1 - 1.71x_L + 0.70x_L^2}. \quad (21)$$

Although, the length of the test section used in the experiments conducted by Ferre (1981) was only 12 m long, they exhibit close agreement with the data derived from the present experimental measurements.

A graphical representation of the experimentally established relationship between the Strouhal number and the Lockhart-Martinelli parameter is shown on the logarithmic plot given on Fig. 27. The Lockhart-Martinelli parameter is defined according to Eqs. (22) and (23) as:

Lockhart–Martinelli parameter,

$$X = \sqrt{\frac{\left(\frac{dp}{dx}\right)_L}{\left(\frac{dp}{dx}\right)_G}} = \sqrt{\frac{f_L \rho_L U_{SL}^2}{f_G \rho_G U_{SG}^2}} \quad (22)$$

Where,

$f_L, f_G, \rho_L, \rho_G, \left(\frac{dP}{dx}\right)_L, \left(\frac{dP}{dx}\right)_G$ represent liquid and gas fugacities, liquid and gas densities and liquid and gas pressure gradients, respectively.

The high Reynolds number asymptote of *f* is a constant. This constant is the same for both *G* and *L*. Therefore $f_g/f_L = 1$.

Thus,

$$X = \sqrt{\frac{\left(\frac{dp}{dx}\right)_L}{\left(\frac{dp}{dx}\right)_G}} = \sqrt{\frac{\rho_L}{\rho_G}} \frac{U_{SL}}{U_{SG}} \quad (23)$$

Fig. 27 illustrates a plot of the dimensionless Strouhal number *St*, defined as $\frac{f_s D}{U_{SG}}$ as a function of the Lockhart-Martinelli parameter as suggested by Azzopardi (1997). Also included on this plot, are experimental data from the present study, compared to data from previous similar experimental studies conducted in horizontal pipes of similar diameter. A comparison of these data sets confirms that

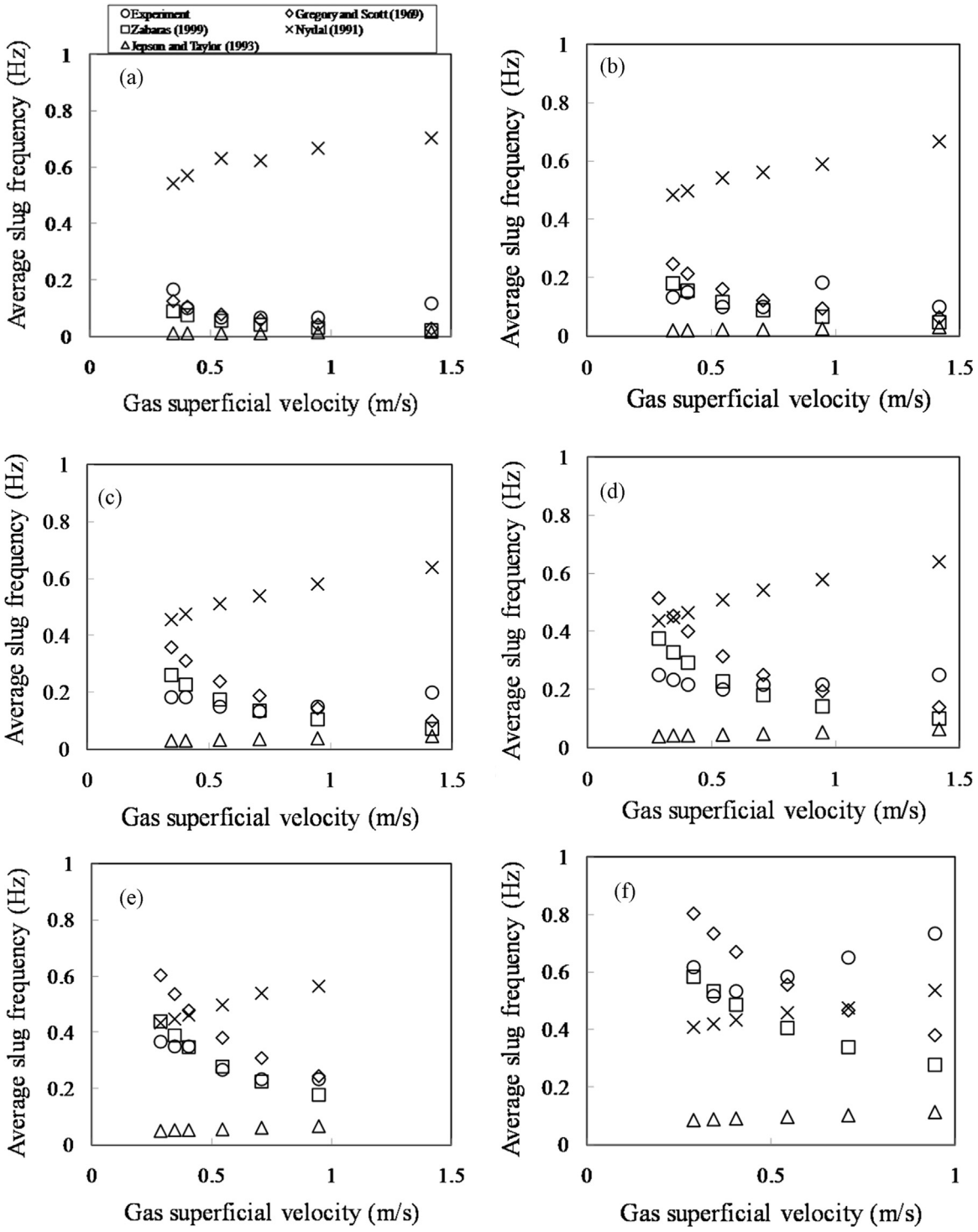

Fig. 24. Plots of the variation of average slug frequency with gas superficial velocity using results obtained from experiments and empirical correlations for the following liquid superficial velocities (m s^{-1}): (a) 0.05 (b) 0.095 (c) 0.14 (d) 0.19 (e) 0.24 (f) 0.38.

the observed flow pattern is slug flow, where the frequency is made dimensionless by dividing by the gas superficial velocity. With the exception of the 50 mm pipe diameter, all of the other data sets may be shown to confirm a satisfactory linear fit with a positive gradient for all of the plotted experimental pipe diameter data sets.

4. Conclusion

The paper has presented an analysis and discussion of the results of a series of experiments conducted to characterize the slug flows produced within a horizontal 6 m long and 67 mm internal diameter pipe when known quantities of air and silicone oil are injected at the inlet of the pipe. The flow characteristics were measured and characterized using advanced instrumentation, including electrical capacitance tomography (ECT), a wire mesh sensor (WMS) and a differential pressure (DP) transducer cell. A summary of the main results are:

(1) The slug flow pattern is fully developed at 4400 mm (64 pipe diameters) upstream of the mixing section based on the

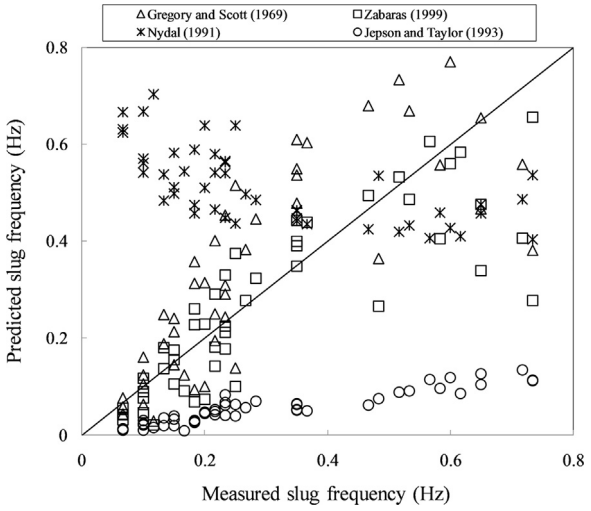

Fig. 25. A plot to compare the experimental data against the results of previously published empirical correlation models.

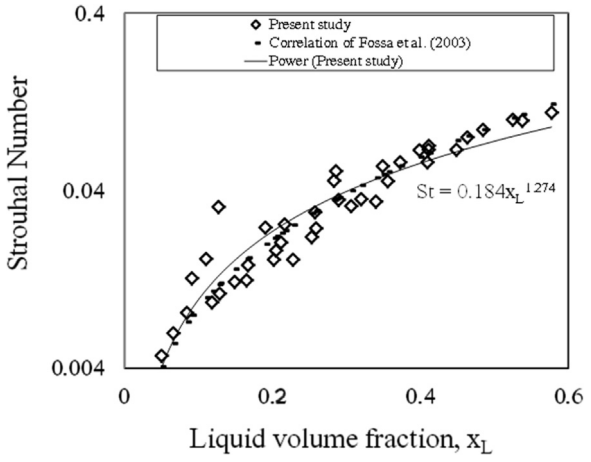

Fig. 26. A logarithmic plot of the dimensionless Strouhal number versus the liquid volume fraction. A comparison of the present experimental data is presented against the predictions derived from the correlation model proposed by Fossa et al. (2003).

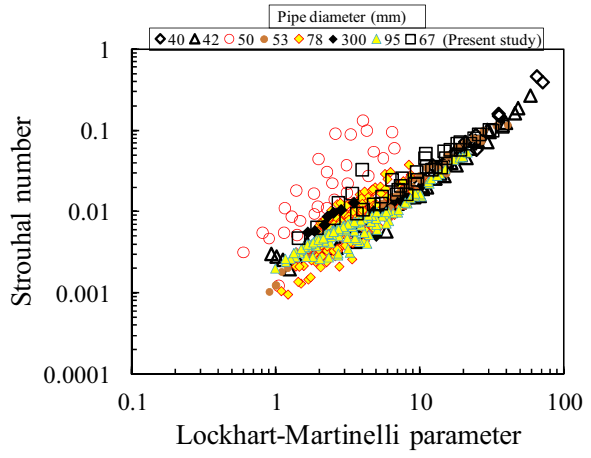

Fig. 27. A plot of dimensionless frequency based on liquid superficial velocity against Lockhart–Martinelli parameter. 40 mm–Fossa et al. (2003); 42 mm –Heywood and Richardson (1979); 50 mm–McNulty (1987); 53 mm–Nydal et al. (1991); 78 mm–Manolis et al. (1990); 300 mm–Jepson and Taylor (1993); 95 mm – Hill and Woods (1990).

evidence provided by a plot of slug frequency against axial distance, an examination of the PDF of void fraction and a comparison between slug front and slug tail velocities for the flow conditions considered.

(2) An examination of the experimental results confirmed for horizontal slug flow, the existence of an expected linear dependence between the slug translational velocity and the mixture superficial velocity. A good agreement was shown between the present experimental data trends and with those predicted by the empirical relationships proposed by Weber (1981) and Bendiksen (1984).

(3) It was found that for horizontal pipes the bubbles exhibit a drift velocity component that far exceeds the value found for vertical riser pipes.

(4) The frictional pressure gradient was observed to increase with liquid and gas superficial velocities.

(5) The average cross-sectional void fraction was observed to increase with an increase in gas superficial velocity.

(6) The void fraction determined for the liquid slugs were found to be almost insensitive to both liquid and gas superficial velocities considered. The void fractions in the elongated bubble were confirmed to increase with an increase in the gas superficial velocity.

(7) No clear relationship was determined to characterize the slug unit in terms of the computed dimensionless slug length or other measured or computed variables. The observed slug lengths were of the order of 8-46 pipe diameters and relatively independent of flow conditions. However, the elongated bubble lengths followed a near linear relationship with the corresponding measured slug unit lengths.

(8) The ratio of average length of liquid slug to the average elongated bubble length, L_S/L_{EB}, decreases as the gas superficial velocities increase and asymptotically approach zero at high gas superficial velocities.

(9) The length of the observed slug unit increases as the gas superficial velocity increases. However, at gas superficial velocity of 0.54 m s^{-1}, the slug unit gets shorter with an increase in liquid superficial velocity. This confirms the observation reported by Hernandez-Perez (2008).

(10) The observed slug frequency increases with an increase in the liquid superficial velocity, whilst the computed dimensionless Strouhal number was found to increase with corresponding increases in the liquid volume fraction and Lockhart–Martinelli parameter. The observed frequency values were in good agreement with those predicted by the empirical correlation proposed by Fossa et al. (2003), whose implicit coefficients were computed from present experimental data. The slug frequencies predicted by the Zabaras (1999) correlation method gave closest agreement to the experimental data.

This study has provided a fundamental insight into the physical phenomena that govern the behaviour of slug flows in horizontal pipes and the parameters that may be employed to characterize the slug flows generated under various flow conditions.

Acknowledgments

M. Abdulkadir would like to express sincere appreciation to the Nigerian government through the Petroleum Technology Development Fund (PTDF) for providing the funding for his doctoral studies.

This work has been undertaken within the Joint Project on Transient Multiphase Flows and Flow Assurance, sponsored by the UK Engineering and Physical Sciences Research Council (EPSRC); Advantica; BP Exploration; CD-adapco; Chevron; ConocoPhillips; ENI; ExxonMobil; FEESA; IFP; Institutt for Energiteknikk; Norsk Hydro; PDVSA (INTERVEP); Petrobras; PETRONAS; Scandpower PT; Shell; SINTEF; Statoil and TOTAL. The Authors wish to express their sincere gratitude for their supports.

References

Abdulkadir, M., Hernandez–Perez, V., Lowndes, I.S., Azzopardi, B.J., Brantson, E.T., 2015. Detailed analysis of phase distributions in a vertical riser using wire mesh sensor (WMS). Exp. Therm. Fluid Sci. 59, 32–42.

Abdulkadir, M., Hernandez–Perez, V., Lowndes, I.S., Azzopardi, B.J., Dzomeku, S., 2014. Experimental study of the hydrodynamic behaviour of slug flow in a vertical riser. Chem. Eng. Sci. 106, 60–75.

Abdulkadir, M., Zhao, D., Azzi, A., Lowndes, I.S., Azzopardi, B.J., 2012. Two-phase air–water flow through a large diameter vertical 180° return bend. Chem. Eng. Sci. 79, 138–152.

Abdulkadir, M., Zhao, D., Sharaf, S., Abdulkareem, L., Lowndes, I.S., Azzopardi, B.J., 2011. Interrogating the effect of 90° bends on air–silicone oil flows using advanced instrumentation. Chem. Eng. Sci. 66, 2453–2467.

Azzopardi, B.J., 1997. Drops in annular two-phase flow. Int. J. Multiph. Flow. 23, S1–S53.

Bendiksen, K.H., 1984. An experimental investigation of the motion of long bubbles in inclined tubes. Int. J. Multiph. Flow. 10, 467–483.

Bagci, S., 2003. An investigation of two-phase slug flow in inclined pipelines. Energy Sources 26, 627–638.

Barnea, D., Brauner, N., 1985. Holdup of liquid slug in two-phase intermittent flow. Int. J. Multiph. Flow. 11, 43–49.

Barnea, D., Taitel, Y., 1993. A model for slug length distribution in gas–liquid slug flow. Int. J. Multiph. Flow. 19, 829–838.

Beggs, H.D., Brill, J.P., 1973. A study of two-phase flow in inclined pipes. Trans. Petrol. Society 256. ASME, pp. 607–617.

Benjamin, T.B., 1968. Gravity current and related phenomena. J. Fluid Mech. 31 (part 2), 224.

Costigan, G., Whalley, P.B., 1997. Slug flow regime identification from dynamic void fraction measurements in vertical air–water flows. Int. J. Multiph. Flow. 23, 263–282.

Crowley, J.C., Sam, R.G., Wallis, G.B., 1984. Slug flow in a large diameter pipe. Paper presented at the AIChE A. Mtg, San Francisco, CA.

da Silva, M.J., Thiele, S., Abdulkareem, L., Azzopardi, B.J., Hampel, U., 2010. High-resolution gas–oil two-phase flow visualization with a capacitance wire-mesh sensor. Flow. Meas. Instrum. 21, 191–197.

Davies, R.M., Taylor, G., 1950. The mechanics of large bubbles rising through extended liquids and through liquids in tubes. Proc. R. Soc. Lond. 200, 375–390.

Dukler, A.E., Hubbard, M.G., 1975. A physical model for gas–liquid slug flow in horizontal and near horizontal tubes. Ind. Eng. Chem. Fundam. 14, 337–347.

Ferre, D., 1981. Ecoulments gas–liquid a poches et a bouchons dans le conduits de section circulaire. These. Inst. National Polytechnic, Toulouse, France.

Fossa, M., Guglielmini, G., Marchitto, A., 2003. Intermittent flow parameters from void fraction analysis. Flow. Meas. Instrum. 14, 161–168.

Franca, F., Lahey, R.T., 1992. The use of drift-flux techniques for the analysis of horizontal two-phase flows. Int. J. Multiph. Flow. 18, 787–801.

Gomez, L.E., Shoham, O., Taitel, Y., 2000. Prediction of slug liquid holdup: horizontal to upward vertical flow. Int. J. Multiph. Flow. 26, 517–521.

Gregory, G.A., Nicholson, M.K., Aziz, K., 1978. Correlation of the liquid volume fraction in the slug for horizontal gas–liquid slug flow. Int. J. Multiph. Flow. 4, 33–39.

Gregory, G.A., Scott, D. S., 1969. Correlation of liquid slug velocity and frequency in horizontal concurrent as liquid flow, 15, 833–835.

Greskovich, E.J., Shrier, A.L., 1972. Slug frequency in horizontal gas–liquid slug flow. Ind. Eng. Chem. Proc. Des. Dev. 11, 317–318.

Hernandez–Perez, V., 2008. Gas–liquid two-phase flow in inclined pipes (PhD Thesis). University of Nottingham.

Hernandez-Perez, V., Abdulkadir, M., Azzopardi, B.J., 2010. Slugging frequency correlation for inclined gas-liquid flow. World Acad. Sci., Eng. Technol. 61, 44–51.

Heywood, N.I., Richardson, J.F., 1979. Slug flow of air–water mixtures in a horizontal pipe: determination of liquid holdup by gamma-ray absorption. Chem. Eng. Sci. 34, 17.

Hill, T.J., Wood, D.G., 1990. A new approach to the predictions of slug frequency. SPE 20629. 65th Annual Technical Conference and Exhibition of the Society of Petroleum Engineers, New Orleans, September 23rd – 26th, 141–149.

Hubbard, M.G., 1965. An analysis of horizontal gas–liquid slug (PhD Thesis). University of Houston.

Hubbard M.G., Dukler A.E., 1966. The characterisation of flow regimes for horizontal two-phase flow. Proceedings of the 1966 Heat Transfer Fluid Mechanics Institute. Stanford University Press, Stanford, 385-400.

Jepson, W.P., Taylor, R.E., 1993. Slug flow and its transitions in large-diameter horizontal pipes. Int. J. Multiph. Flow. 19, 411–420.

Khatib, Z., Richardson, J.F., 1984. Vertical co-current flow of air and shear thinning suspensions of kaolin. Chem. Eng. Res. Des. 62, 139–154.

Kouba, G. E., 1986. Dynamic calibration of two types of capacitance sensors used in measuring liquid holdup in two-phase. Proceedings of the 32nd ISA International, Seattle.

Malnes, D., 1983. Slug flow in vertical, horizontal and inclined pipes. IFE/KR/E-83/002 Institute for Energy Technology, Kjeller, Norway.

Manolis, I.G., Mendes–Tatsis, M.A., Hewitt, G.F., 1990. The effect of pressure on slug frequency The effect of pressure on two-phase horizontal flow. Proceedings of the 2nd International Conference on Multiphase Flow, Kyoto, 2, 1F1–35–40.

Marcano, R., Sarica, T.X., Brill, J. P, C., 1998. A Study of slug characteristics for two-phase horizontal flow. Soc. Pet. Eng. (SPE) 39856, 214.

McNulty, J.G., 1987. Fluid property effects of Freon two-phase flow in a horizontal pipeline. Proceedings of the 2nd International Conference on Multiphase Flow (BHRA Pub.), 149–160.

Nicholson, K., Aziz, K., Gregory, G.A., 1978. Intermittent two phase flow in horizontal pipes, predictive models. Can. J. Chem. Eng. 56, 653–663.

Nydal, O.J., Pintus, S., Andreussi, P., 1991. Statistical characterization of slug flow in horizontal pipes. Int. J. Multiph. Flow. 18, 439–453.

Sakaguchi, T., Ozawa, M., Hamaguchi, H., Nishiwaki, F., Fujii, E., 1987. Analysis of the impact force by a transient liquid slug flowing out of a horizontal pipe. Nucl. Eng. Des. 99, 63–71.

Shoham, O., 2006. Mechanistic modelling of gas–liquid two-phase flow in pipes, University of Tulsa, Society of Petroleum Engineers, USA.

Taitel, Y., Dukler, A.E., 1977. A model for slug frequency during gas–liquid flow in horizontal and near horizontal pipes. Int. J. Multiph. Flow. 3, 585–596.

Ujang, P.M., Lawrence, C.J., Hale, C.P., Hewitt, G., 2006. Slug initiation and evolution in two-phase horizontal flow. Int. J. Multiph. Flow. 32, 527–552.

Weber, M.E., 1981. Drift in intermittent two-phase flow in horizontal pipes. Can. J. Chem. Eng. 59, 398–399.

Weisman, J., Duncan, D., Gibson, J., Crawford, T., 1979. Effects of fluid properties and pipe diameter on two-phase flow patterns in horizontal lines. Int. J. Multiph. Flow. 5, 437–462.

Woods, B.D., Hanratty, T.J., 2006. Frequency and development of slugs in a horizontal pipe at large liquid flows. Int. J. Multiph. Flow. 32, 902–925.

Zabaras, G.J., 1999. Prediction of slug frequency for gas/liquid flows. Soc. Pet. Eng. (SPE) 5, 252–258.

Zheng, G.H., Brill, J.P., Shoham, O., 1994. Slug flow behaviour in a hilly terrain pipelines. Int. J. Multiph. Flow. 20, 63–79.